JOURNAL OF MATERIALS SCIENCE 24 (1989) 2581–2586

Microstructure development in Sb_2O_3-doped ZnO

JINHO KIM, TOSHIO KIMURA, TAKASHI YAMAGUCHI
Faculty of Science and Technology, Keio University, Yokohama, Japan

The microstructure development in Sb_2O_3-doped ZnO was studied at doping levels up to 2.0 mol %. Dopant Sb_2O_3 reacted with ZnO to form inclusion particles, α-$Zn_7Sb_2O_{12}$, and inhibited the grain growth of ZnO. With increasing doping level of Sb_2O_3, the growth rate of ZnO decreased whereas that of inclusion particles increased. Some inclusion particles were trapped in ZnO grains at low doping levels of Sb_2O_3, but the volume fraction of trapped inclusion particles decreased with increasing doping level. Stereological analysis of the size and number ratios of ZnO grains and inclusion particles indicated that a compatible assumption is needed to evaluate Zener effect in two-phase sintering.

1. Introduction

This study is a part of a research project to better understand the sintering mechanism in ZnO varistor systems. The previous study [1] on the mechanism of reaction and densification in Sb_2O_3-doped ZnO showed that the second phase, α-$Zn_7Sb_2O_{12}$, plays an important role in the microstructure development. The purpose of this work was to study the effect of inclusion particles on the grain growth of ZnO as a function of Sb_2O_3-doping level and also to understand the two-phase sintering by stereological analysis.

Zener [2] studied the effect of inclusion particles on the grain growth in polycrystalline materials. The limiting grain size (D) of the host phase is given by

$$D = 2d/3f \quad (1)$$

where d and f are the average size and volume fraction of inclusion particles, respectively. This equation assumes that the maximum drag force on the grain boundary by an inclusion particle is $\pi/2d\gamma_{gb}$, where γ_{gb} is the grain-boundary energy, and also that the grain boundary stops moving when the drag force balances the driving force $2\gamma_{gb}/D$. However, some authors [3] pointed out that the driving force for grain growth is overestimated. In fact, many experimental results indicated that the observed grain sizes are much smaller than those predicted by this relation. Hence, modified relations [3–6] have been suggested, which, however, have not been fully tested experimentally for ceramic materials. In addition, the test of Zener effect has been confined to stabilized microstructures in which grain growth stops or constant grain/particle size ratio [7] prevails in extended heating. However, these conditions do not always hold. Thus, the role of inclusion particles in microstructure development has not yet been fully evaluated.

A more careful observation on the variation of grain/particle size ratio and the behaviour of inclusion particles in grain growth is needed for better understanding of the sintering mechanism when inclusions are present. Stereological analysis has been used for this purpose. Two stereological relations can be applied depending on the dispersion state of inclusion particles throughout the microstructure development (see Appendix for the derivation)

$$\log [N_A(i)/N_A(h)] = m(f) + 2\log (\bar{D}_h/\bar{d}_i) \quad (2)$$

$$\log [N_A(i)/N_A(h)] = n(f) + \log (\bar{D}_h/\bar{d}_i) \quad (3)$$

where $N_A(h)$ and $N_A(i)$ are the number of grains and inclusion particles with average sizes of $\bar{D}_h$ and $\bar{d}_i$ in unit area, respectively. The term $m(f)$ and $n(f)$ is a function of volume fraction f of a second phase. Equation 2 is applicable when almost all inclusion particles move with the grain boundaries, and Equation 3 is valid when the mobility of inclusion particles is sufficiently low to be trapped within the matrix grains.

In the observation on the microstructure of Sb_2O_3-doped ZnO, the evaluation of the slope in the plot of $\log N_A(i)/N_A(h)$ against $\log \bar{D}_h/\bar{d}_i$ by the above mentioned criteria, has enabled us to explain the microstructure development in the system ZnO–Sb_2O_3 with respect to the amount of inclusions.

2. Experimental techniques

Properties of raw materials and the method of sample preparation are described in our previous paper [1]. Discs with densities of $3.00 \pm 0.02\,g\,cm^{-3}$ were preheated at 500° C for 1 h, and fired between 1200 and 1400° C for appropriate time periods. The relative density of fired discs was determined by the water-immersion method, in which 5.78 and $6.24\,g\,cm^{-3}$ were used for ZnO and α-$Zn_7Sb_2O_{12}$, respectively.

Microstructures of polished and thermally etched specimens were examined with a scanning electron microscope (SEM). The average grain size was determined in SEM photographs by taking 1.45 times the mean chord length obtained by the line-intercept method [8]. The grain-size distribution of ZnO was obtained by Cahn and Fullman's method [9]. The

0022–2461/89 $03.00 + .12

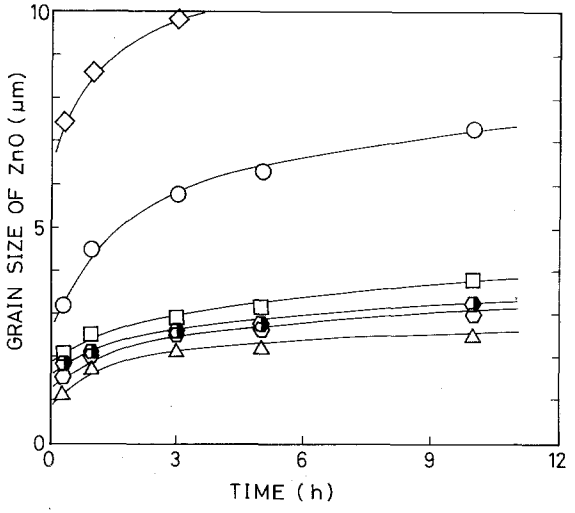

Figure 1 Effect of doping level of Sb_2O_3 on the grain growth of ZnO, heated at 1300° C. Doped with coarse Sb_2O_3 (4.1 μm): (◇) 0, (○) 0.1, (□) 0.5, (⬡) 1.0, (△) 2.0 mol %, and with fine Sb_2O_3 (1.2 μm): (◑) 1.0 mol %.

particle size of inclusions was determined by taking $\pi/2$ times the mean section diameter after Fullman [10]. About 1000 and 300 chords were recorded for ZnO and inclusion particles, respectively. The relation between the numbers of ZnO grains and inclusion particles was derived by direct counting on SEM screens. More than 300 ZnO grains were counted.

3. Results and discussion

3.1. Effect of Sb_2O_3 on the densification and grain growth

Fig. 1 shows isothermal grain growth of Sb_2O_3-doped ZnO at 1300° C. The grain size of ZnO decreases with increasing doping level, but little effect of Sb_2O_3 particle size was observed. The formation reaction of α-$Zn_7Sb_2O_{12}$ was rapid and was completed in 10 min at 1300° C. Thus, the effect of Sb_2O_3 doping level on the grain growth of ZnO is explained by the amount of the second phase, α-$Zn_7Sb_2O_{12}$.

Figs 2 and 3 show the grain size of Sb_2O_3-doped ZnO as a function of relative density for coarse

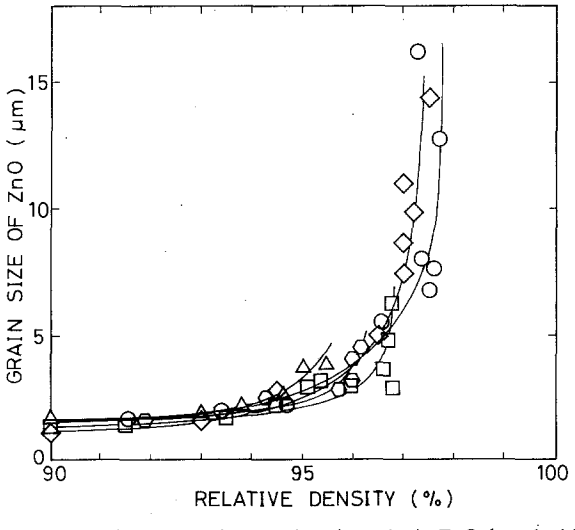

Figure 2 Densification–grain growth trajectories in ZnO doped with coarse Sb_2O_3 (4.1 μm). (◇) No addition, (○) 0.1, (□) 0.5, (⬡) 1.0 and (△) 2.0 mol %.

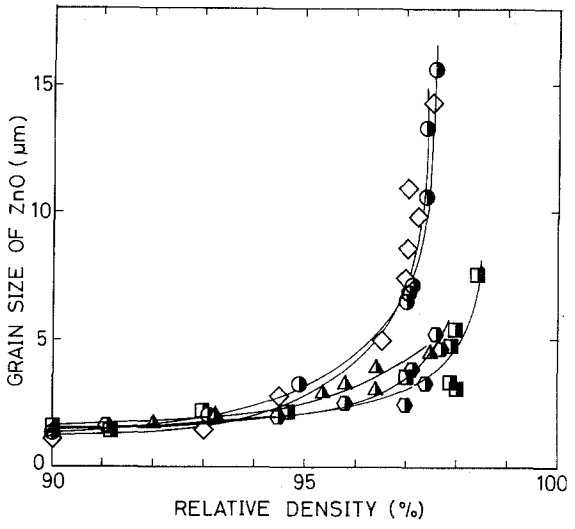

Figure 3 Densification–grain growth trajectories in ZnO doped with fine Sb_2O_3 (1.2 μm). (◇) No addition, (◑) 0.1, (◨) 0.5, (◑) 1.0 and (▲) 2.0 mol %.

(4.1 μm) and fine (1.2 μm) Sb_2O_3, respectively. The relative density in the final stage of sintering decreases with increasing doping level for coarse Sb_2O_3. For fine Sb_2O_3, on the other hand, the relative density in the final stage for 0.5 mol % addition is higher than that for 0.1 mol % addition, and further addition decreases the density gradually.

Addition of 0.1 mol % Sb_2O_3 had little effect on the grain growth of ZnO regardless of the particle size of Sb_2O_3. Consequently, rapid grain growth occurs in the intermediate and final stages of sintering as in pure ZnO. The grain growth of ZnO becomes sluggish with increasing doping level in these stages, implying that extended sintering time or higher temperature is needed to achieve high density for increased amounts of the second phase.

3.2. Effect of Sb_2O_3 on the microstructure and grain-size distribution

Fig. 4 shows the effect of particle size of Sb_2O_3 on the microstructure of ZnO containing 1.0 mol % Sb_2O_3. Large pores are observed in ZnO containing coarse Sb_2O_3, while a dense microstructure is obtained for fine Sb_2O_3. These pores were generated by the vapour-phase reaction of Sb_2O_3 with ZnO during firing, and retained in the final stage of sintering. The behaviour of pores explains the decrease in relative density with increasing doping level as shown in Fig. 2. Regardless of the particle size of Sb_2O_3, almost the same sizes of ZnO grains and inclusion particles were obtained. Thus, the large pores are thought to have little effect on the microstructure development. Therefore, only the results for ZnO doped with coarse Sb_2O_3 will be presented and discussed hereafter.

Fig. 5 illustrates the microstructures of Sb_2O_3-doped ZnO heated at 1400° C for 2 h. Because extended heating did not increase the grain size of ZnO doped with more than 0.5 mol % Sb_2O_3, 1400° C–2 h heating was appropriate to obtain stabilized microstructures.

Inclusion particles exist within ZnO grains as well as on the grain boundaries, and micropores were observed in ZnO grains with 0.1 mol % addition of Sb_2O_3. In ZnO doped with 0.5 mol % Sb_2O_3, practically no

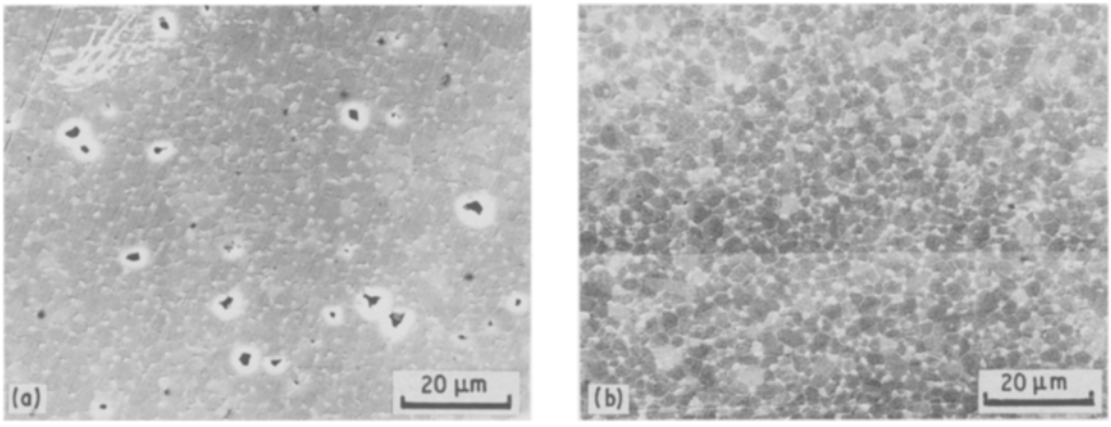

Figure 4 Effect of particle size of Sb_2O_3 on the microstructure of Sb_2O_3-doped ZnO. Doped with 1.0 mol % of (a) coarse (ZS_c 1.0) and (b) fine (ZS_f 1.0) Sb_2O_3, heated at 1300° C for 10 h.

pores were observed in ZnO grains, and most inclusions are located at three or four grain junctions and some of them are present in ZnO grains. In ZnO doped with 1.0 and 2.0 mol % Sb_2O_3, most inclusion particles are located at three or four grain junctions. Clustering of inclusion particles [11] was observed in ZnO with 2.0 mol % Sb_2O_3.

The spherical shape of pores and inclusion particles observed in ZnO grains with 0.1 mol % addition Sb_2O_3 implies that they were trapped during grain growth of ZnO. The micropores are thought to decrease the relative density of ZnO doped with less than 0.5 mol % Sb_2O_3 as compared with that containing 0.5 mol % or more Sb_2O_3 (see Fig. 3). The preference of inclusion particles to three or four grain junctions is determined by the interfacial energies. In ZnO doped with 0.1 mol % Sb_2O_3, however, the long diffusion paths along grain boundaries keep inclusion particles away from these junctions.

Fig. 6 illustrates the effect of Sb_2O_3 on the grain size distribution of ZnO. In this plot, the standard deviation (σ_g) in the cumulative log-normal distribution [12] was used as a criterion of grain-size distribution. The grain-size distribution of pure ZnO became narrow as grain growth proceeded. A similar tendency was observed in ZnO doped with 0.5 and 1.0 mol % Sb_2O_3. With 2.0 mol % Sb_2O_3, ZnO always showed a narrow grain-size distribution. With 0.1 mol % Sb_2O_3, on the other hand, the grain-size distribution broadened in the final stage of sintering. No abnormal grain

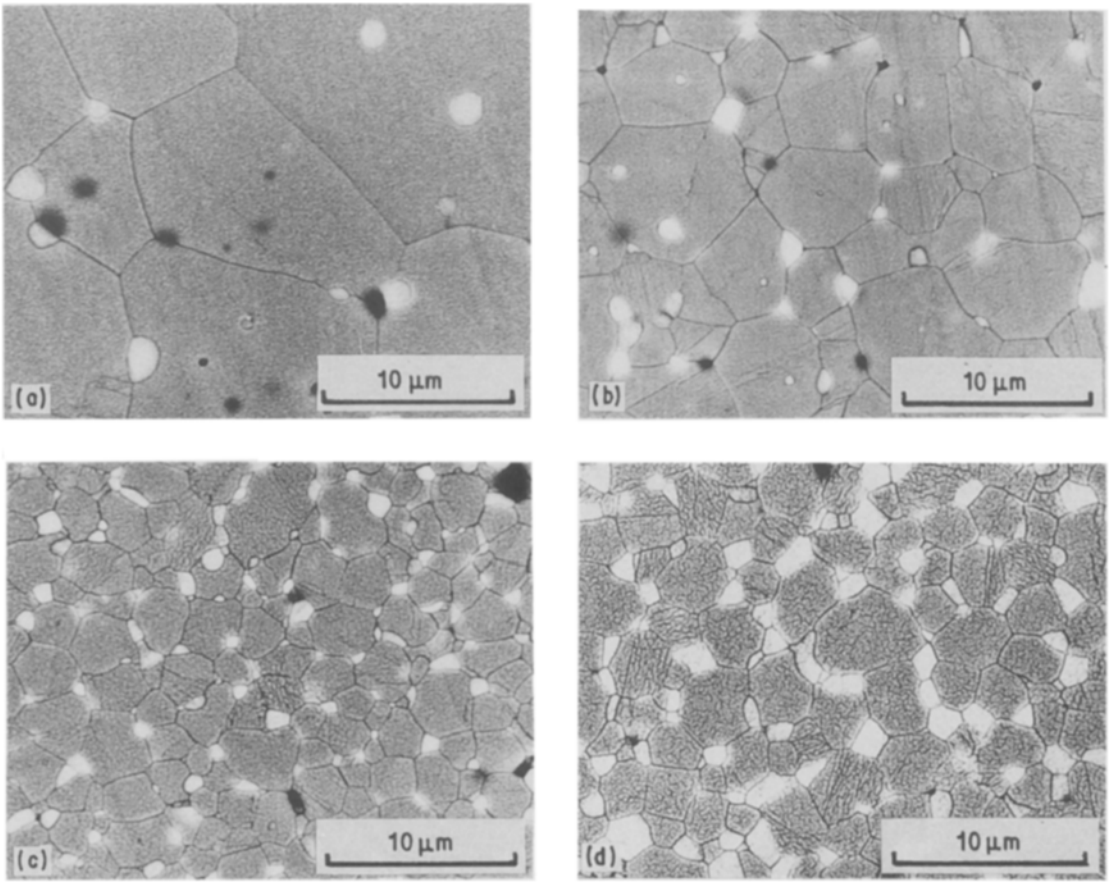

Figure 5 Effect of doping level of Sb_2O_3 on the microstructure of Sb_2O_3-doped ZnO, heated at 1400° C for 2 h. (a) 0.1, (b) 0.5, (c) 1.0 and (d) 2.0 mol %.

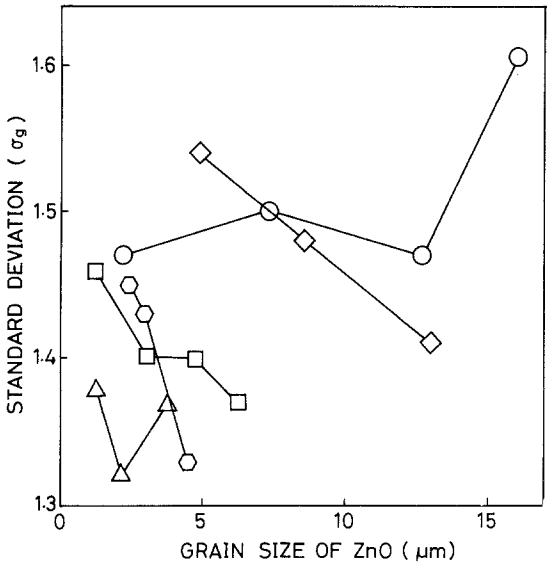

Figure 6 Effect of Sb_2O_3 doping level on the size distribution of ZnO grains. Standard deviation (σ_g) is the ratio of $D_{15.87}$ to D_{50}, where D_R is the grain size with the residue percentage, R, in the cumulative log-normal size distribution curve. (◇) 0, (○) 0.1, (□) 0.5, (⬡) 1.0 and (△) 2.0 mol %.

growth was observed under the conditions studied in this work.

The growth of large grains at the expense of smaller ones should narrow the size distribution as grain growth proceeds in pure ZnO. The dopant Sb_2O_3 narrows the grain size distribution of ZnO by suppressing the grain growth of ZnO in a controlled manner throughout the sintering process. Perhaps local compositional inhomogeneity is responsible for the partial grain-boundary movement which broadens the size distribution in ZnO with 0.1 mol % Sb_2O_3.

3.3. Behaviour of inclusion particles in grain growth

Dopant Sb_2O_3 reacts with ZnO to form α-$Zn_7Sb_2O_{12}$, which develops as a second phase on heating. In this reaction, 0.1, 0.5, 1.0 and 2.0 mol % Sb_2O_3 correspond to about 1, 5, 10 and 20 vol % α-$Zn_7Sb_2O_{12}$, respectively. Hence, volume fraction f of α-$Zn_7Sb_2O_{12}$ will be used instead of Sb_2O_3 doping level in discussing the effect of the amount of inclusion particles on the microstructure development.

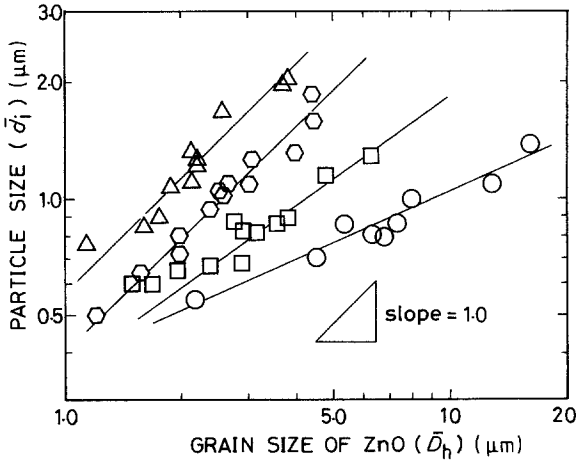

Figure 7 Coalescence of inclusion particles in grain growth of Sb_2O_3-doped ZnO for different volume fractions (f) of α-$Zn_7Sb_2O_{12}$: (○) 0.01, (□) 0.05, (⬡) 0.1 and (△) 0.2.

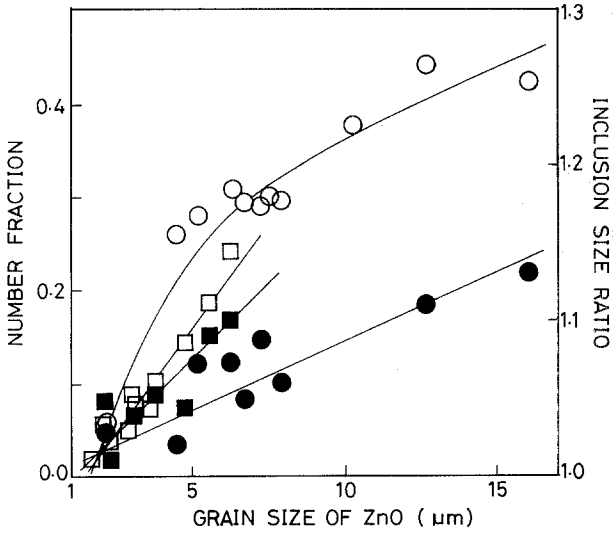

Figure 8 Changes in number fraction (○, □) of inclusion particles trapped in ZnO grains and particle size of inclusions (●, ■) on the grain boundaries relative to those of total inclusions: (○, ●) f = 0.01, (□, ■) f = 0.05.

Fig. 7 shows the coalescence of inclusion particles in grain growth of Sb_2O_3-doped ZnO. For all the amounts of the second-phase studied, inclusion particles grew by coalescence as ZnO grains grew. The slopes of log $\bar{d}_i$–log $\bar{D}_h$ curves were nearly unity in ZnO with volume fractions of second phase of 0.1 and 0.2 (1.0 and 2.0 mol % Sb_2O_3, respectively), where $\bar{d}_i$ and $\bar{D}_h$ are the average sizes of inclusion particles and grain, respectively. With f of 0.05 (0.5 mol % Sb_2O_3), however, the slope was somewhat smaller than unity and much smaller with f of 0.01 (0.1 mol % Sb_2O_3).

The slope of unity means that grain growth proceeds in a normal mode; all inclusion particles are subject to motion with the grain boundaries of ZnO, and their growth rate is almost the same as that of ZnO grains with f = 0.1 and 0.2. For a slope less than unity, on the other hand, grain growth proceeds while inclusion particles are continuously trapped in ZnO grains with f = 0.01 and 0.05.

Fig. 8 shows the changes in the number fraction of inclusion particles trapped within ZnO grains and the ratio of particle size of inclusions on the grain boundaries to total average size of inclusion particles with microstructure development. The data were obtained on section planes. For f = 0.01 and 0.05, the number fraction of inclusion particles increased with grain size of ZnO, and was always much larger with f = 0.01 under the same sintering condition. With f > 0.05, the number fraction was nearly zero throughout the microstructure development. The ratio of particle size increased with increasing grain size of ZnO with f = 0.01 and 0.05. This fact, in other words, means that the coalescence and trapping of inclusion particles occur simultaneously.

The stereological relation between ZnO grain and inclusion particles is illustrated in Fig. 9. In grain growth of Sb_2O_3-doped ZnO from 2.0 μm to respective stabilized sizes, grain/particle size ratios ($\bar{D}_h/\bar{d}_i$) increased about 3 and 2 times with f = 0.01 and 0.05, respectively, and fluctuated in small ranges with f = 0.1 and 0.2. In the meanwhile, the number of particles to number of grains ratios on section planes

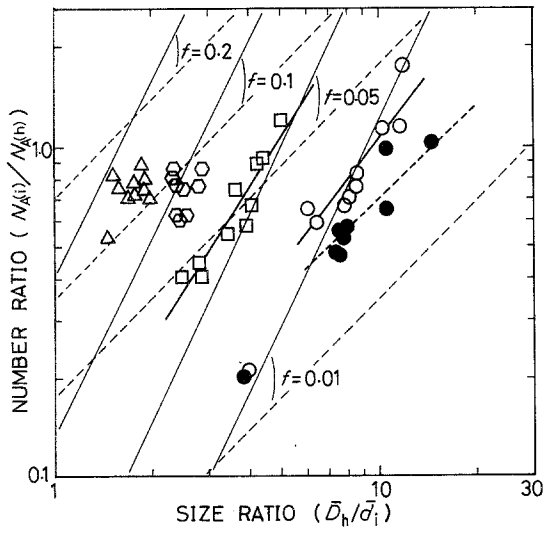

Figure 9 Stereological relation between ZnO grains and inclusion particles. $N_A(i)$ and $\bar{d}_i$ = number and average size of inclusion particles in unit section area, respectively, and $N_A(h)$ and $\bar{D}_h$ = those of ZnO grains, respectively. Total volume fraction (f), (○, ●) 0.01, (□) 0.05, (◯) 0.1 and (△) 0.2; (●) inclusion particles on ZnO grain boundaries. (——) Equation 2, (– – –) Equation 3.

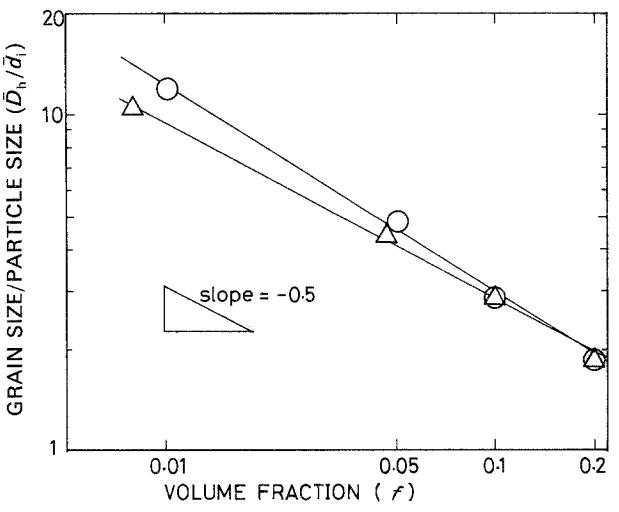

Figure 10 Evaluation of Zener effect for stabilized microstructure of Sb_2O_3-doped ZnO, heated at 1400° C for 2 h. (○) Total inclusion particles, (△) particles on the grain boundaries.

($N_A(i)/N_A(h)$) increased about 9, 3, 1.5 and 1.3 times with f = 0.01, 0.05, 0.1 and 0.2, respectively. Thus, the slope of the plot with f = 0.01 was between 2 (Equation 2) and 1 (Equation 3), and gave a value somewhat smaller than 2 with f of 0.05. For f = 0.1 and 0.2, the number ratios have not been correlated with the size ratios from the plots.

The increase in the ratios $\bar{D}_h/\bar{d}_i$ and $N_A(i)/N_A(h)$ with increasing grain size with f = 0.01 implies unstable microstructure development; inclusion particles move with ZnO grain boundaries while some of them are trapped continuously within ZnO grains, and the chance of particle coalescence is small, because of the long diffusion distance through the grain boundaries. Thus, the slope of the plot takes a value between 1 and 2. The same plot for the inclusion particles located only on the grain boundaries also gave a slope other than 2, because their volume fraction decreased gradually with increasing ZnO grain size and the derivation of this f value was very difficult. With f = 0.05, ZnO grains grow faster than inclusion particles, so that the microstructure develops unstably throughout the sintering stages. As the number fraction of inclusion particles trapped in ZnO grains is less than 0.2 (See Fig. 8), the slope takes a value close to 2. With f = 0.1 and 0.2, all inclusion particles move with the grain boundaries and coalesce during sintering. As the growth rate of ZnO grains was almost the same as that of inclusion particles, $\bar{D}_h/\bar{d}_i$ became roughly constant in microstructure development. A small increase in the number ratio is perhaps due to the local inhomogeneity in the dispersion of inclusion particles.

3.4. Evaluation of the Zener effect

To evaluate the Zener effect for stabilized microstructure of Sb_2O_3-doped ZnO, the grain/particle size ratio was plotted against the volume fraction, f, of inclusion particles according to the following equation;

$$\bar{D}_h/\bar{d}_i = Cf^m \quad (4)$$

where C and m are a constant and exponent, respectively. The results are shown in Fig. 10. For comparison, the same relation for the inclusion particles only on the grain boundaries calculated from the data in Fig. 8, was also plotted. The constant C and exponent m were obtained by the least square method and compared with those predicted in several relations in Table I. The exponent (0.62) for the overall inclusion particles is larger than Gladmans value of 0.5 [5], and the constant (0.71) is smaller than the constants in the equations with the exponent equal to 0.5. The exponent (0.53) obtained by compensated $\bar{d}_i$ and f, on the other hand, is nearly 0.5, and the constant (0.83) is close to those obtained by Haroun and Budworth (1.03) and Gladman (0.88) [3, 5].

The discrepancy of the former relation from several predicted ones is attributed to the variation of the dispersion state of inclusion particles with their volume fraction, f, which makes the assumption unacceptable.

4. Conclusions

In the sintering of Sb_2O_3-doped ZnO, the grain growth of ZnO is sluggish and the stabilized grain size decreases with increasing doping level.

Inclusion particles grow by coalescence, and their

TABLE I Comparison of experimental results with modified Zener relations in Sb_2O_3-doped ZnO

Model	C	$-m$	Comment
Zener [2]	0.67	1.0	Random distribution of
Haroun [3]	0.08	1.0	inclusion particles
	2.06	0.5	One particle per grain boundary
Zener [2]	1.97	0.5	Revised form using
Haroun [3]	1.03	0.5	Anand's relation [4]
Gladman [5]	0.88	0.5	$Z \simeq 2$ in this study
Hellman [6]	1.82	0.33	All particles located at grain corners
This study	0.71	0.62	Considering total particles
This study	0.83	0.53	Taking particles only on the grain boundaries

growth rate increases with increasing amount of second phase, α-$Zn_7Sb_2O_{12}$.

For the volume fraction, f, of inclusion particles equal to 0.05 or less, inclusion particles are trapped continuously in ZnO grains, resulting in a decrease in the amount of inclusions responsible for growth inhibition. For $f > 0.05$, however, practically all inclusion particles move with the grain boundaries.

The stereological analysis of the relation between the sizes and the numbers of ZnO grains and inclusion particles showed that an assumption compatible with the variation in the amount of second phase is needed in the evaluation of Zener effect in two-phase sintering.

Appendix

For a grain of a truncated octahedron with an edge length of l, the following relations [5] are obtained between grain size ($\bar{D}_h$), volume (V), surface area (A) and grain-boundary area per unit volume (S_V)

$$\bar{D}_h = \sqrt{6}l \quad \text{(A1)}$$

$$V = 4\sqrt{3}/9\bar{D}_h^3 \quad \text{(A2)}$$

$$A = (1 + 2\sqrt{3})\bar{D}_h^2 \quad \text{(A3)}$$

$$S_V = \tfrac{1}{2}A/V = 2.9\bar{D}_h^{-1} \quad \text{(A4)}$$

In a section plane, the mean intercept area ($\bar{A}$) and length ($\bar{L}$) of random test lines are

$$\bar{A} = 3.77l^2 = 0.628\bar{D}_h^2 \quad \text{(A5)}$$

$$\bar{L} = \bar{D}_h/1.45 \quad \text{(A6)}$$

Case 1

For a polycrystalline material with second-phase inclusion, if all the inclusion particles move with the grain boundaries in microstructure development, the number of inclusion particles per unit volume ($N_V(i)$) is

$$N_V(i) = 6f/\pi\bar{d}_i^3 \quad \text{(A7)}$$

where f and $\bar{d}_i$ are the volume fraction and the average size of inclusion particles, respectively. As $V_V = A_A$ by stereology, the number of the matrix grains per unit section area ($N_A(h)$) and that of inclusion particles ($N_A(i)$) are given as follows

$$N_A(h) = (1 - f)/\bar{A} = (1 - f)/0.628\bar{D}_h^2 \quad \text{(A8)}$$

$$N_A(i) = (6f/\pi\bar{d}_i^3)\bar{d}_i = 6f/\pi\bar{d}_i^2 \quad \text{(A9)}$$

Hence, the ratio of $N_A(i)$ to $N_A(h)$ becomes

$$N_A(i)/N_A(h) \simeq [1.2f/(1 - f)](\bar{D}_h/\bar{d}_i)^2 \quad \text{(A10)}$$

As the term $1.2f/(1 - f)$ is constant for a given volume fraction f, the above equation is rewritten as follows

$$\log [N_A(i)/N_A(h)] = m(f) + 2 \log (\bar{D}_h/\bar{d}_i) \quad \text{(A11)}$$

In fully dense polycrystalline materials, if $\bar{d}_i \propto \bar{D}_h$, $\log (\bar{D}_h/d_i)$ is constant and the right-hand side of Equation A11 is a function only of volume fraction, f.

Case 2

In the case where inclusion particles are trapped continuously in the matrix grains as the grain grows, the effective volume fraction, f_e, defined as the volume fraction of the second phase on the grain boundaries, is shown as

$$f_e = fS_V\bar{d}_i \simeq 2.9f(\bar{d}_i/\bar{D}_h) \quad \text{(A12)}$$

Substituting the effective volume fraction, f_e, for f in Equation A11, and taking the denominator $1 - f_e$ as unity, assuming $f_e \ll 1$ the resultant equation is

$$\log [N_A(i)/N_A(h)] = \log 3.48f + \log (\bar{D}_h/\bar{d}_i)$$
$$= n(f) + \log (\bar{D}_h/\bar{d}_i) \quad \text{(A13)}$$

References

1. J. H. KIM, T. KIMURA and T. YAMAGUCHI, *J. Mater. Sci.* in press (1989).
2. C. S. SMITH, *Trans. AIME* **175** (1948) 15.
3. N. A. HAROUN and D. W. BUDWORTH, *J. Mater. Sci.* **3** (1968) 326.
4. L. ANAND and J. GURLAND, *Metall. Trans.* **A6** (1975) 928.
5. T. GLADMAN, *Proc. R. Soc. London* **A294** (1966) 298.
6. P. HELLMAN and M. HILLERT, *Scand. J. Metall.* **4** (1975) 211.
7. S. HORI, R. KURITA, M. YOSHIMURA and S. SŌMIYA, *J. Mater. Sci. Lett.* **4** (1985) 1067.
8. W. ROSTOKER and J. R. DVORAK, in "Interpretation of Metallographic Structure" (Academic, New York, 1977) p. 213.
9. J. W. CAHN and R. L. FULLMAN, *Trans. AIME* **206** (1956) 610.
10. R. L. FULLMAN, *ibid.* **197** (1953) 447.
11. F. F. LANGE and M. M. HIRLINGER, *J. Amer. Ceram. Soc.* **67** (1984) 164.
12. T. HATCH and S. CHOATE, *J. Franklin Inst.* March (1929) 369.

Received 26 April
and accepted 8 September 1988